Biophysical Journal, Volume 96

Supporting Material

A Nebulin Ruler Does Not Dictate Thin Filament Lengths

Angelica Castillo, Roberta Nowak, Kimberly P. Littlefield, Velia M. Fowler, and Ryan S. Littlefield

SUPPLEMENTAL METHODS

Estimation of Nebulin Repeats and Molecular Weight

The number of nebulin repeats in each muscle was estimated by dividing the nebulin length by the repeat distance of a single nebulin actin-binding module (5.5 nm, Supplemental Table 2). Nebulin mol wt was estimated by multiplying the estimated number of modules by the average nebulin module mol wt (4.1 kD, Supplemental Table 2). The average nebulin module mol wt was determined from the complete genomic sequences of human (S6) and mouse (S7) nebulin and from the partial genomic sequence of rabbit nebulin (Supplemental Figure 1C). Each complete sequenced exon encoding only nebulin modules were normalized according to the number of encoded modules (1 – 3). The average nebulin module mol wt was identical for all three species.

Image Analysis

To precisely determine the location of NebN and Tmod epitopes, and the extent of phalloidin binding with respect to neighboring Z-lines, we used distributed deconvolution image analysis to determine the 1-D distribution of fluorescence intensity along the thin filament arrays. This method determines parameter values for a single thin filament array which, when repeated along a myofibril, most closely describes the observed fluorescence intensity along the myofibril (5). This method accurately determines epitope locations and thin filament lengths independent of sarcomere lengths using distinct thin filament array models (e.g. for Tmod and phalloidin). For NebN and Tmod myofibril images, we used a 'P-end' model (5) which allows for specific, symmetric staining distally located away from Z-lines (i.e. at or near thin filament P-ends) (Supplemental Figure 2). This model allows for variable intensities of distal staining intensity

relative to the rest of the thin filament and the Z-line. The length parameter corresponds to distance between the center of the distal peak in intensity and the Z-line at the center of the thin filament profile array. For some myofibrils exhibiting relatively high levels of non-specific Tmod staining at Z-lines, we allowed an additional parameter to vary during the fitting procedure to account for this. For phalloidin staining, we used a 'uniform' model (5) which allow for symmetric continuous staining along the thin filament. This model allows for additional intensity at the Z-line relative to the uniform intensity due to thin filament overlap. The length parameter determines the extent phalloidin binding extends away from the Z-line at the center of the thin filament profile and corresponds approximately to the location of half-maximal intensity of the uniformly-stained shoulders.

From the set of 6 rabbits, 7 muscles, and 3 probes, we determined 3412 independent length parameters consisting of 886 NebN lengths, 1076 Tmod lengths, and 1450 Phall lengths. Of these, 60% (532) of the NebN lengths and 82% (879) of the Tmod lengths were paired with Phall lengths corresponding to the same myofibril image region (linescan). For some myofibrils showing prominent non-uniform staining, it was not possible to analyze the fluorescence distribution using this model. In addition, we did not analyze NebN or Tmod staining from myofibrils in which doublets were unresolved or phalloidin staining from myofibrils in which an H-zone was not visible. The results from the analysis constitute 63 total datasets (out of 105 possible), each of a specific probe from a single rabbit muscle. Fitting errors were low for all myofibrils analyzed (median error values for different muscles ranged from 3.13 – 5.30 % for NebN, 4.16 – 6.62 % for Tmod, and 3.41 – 6.65 % for phalloidin) indicated that the fluorescent staining patterns of Tmod, NebN, and phalloidin along myofibrils were consistent with being composed of a single thin filament array profile. The length parameters obtained from the

distributed deconvolution analysis for NebN and Tmod in all seven muscles are shown as histograms in Figure 2 and summarized in Table I.

SUPPLEMENTAL REFERENCES

S1. Schachat, F.H., A.C. Canine, M.M. Briggs, and M.C. Reedy. 1985. The presence of two skeletal muscle alpha-actinins correlates with troponin-tropomyosin expression and Z-line width. *J Cell Biol*. 101:1001-8.

S2. Labeit, S., and B. Kolmerer. 1995. The complete primary structure of human nebulin and its correlation to muscle structure. *J Mol Biol*. 248:308-15.

S3. Labeit, S., and B. Kolmerer. 1995. Titins: giant proteins in charge of muscle ultrastructure and elasticity. *Science*. 270:293-6.

S4. Trinick, J. 1996. Titin as a scaffold and spring. Cytoskeleton. *Curr Biol.* 6:258-60.

S5. Squire, J.M. 1997. Architecture and function in the muscle sarcomere. *Curr Opin Struct Biol.* 7:247-57.

S6. Donner, K., M. Sandbacka, V.L. Lehtokari, C. Wallgren-Pettersson, and K. Pelin. 2004. Complete genomic structure of the human nebulin gene and identification of alternatively spliced transcripts. *Eur J Hum Genet*. 12:744-51.

S7. Kazmierski, S.T., P.B. Antin, C.C. Witt, N. Huebner, A.S. McElhinny, S. Labeit, and C.C. Gregorio. 2003. The complete mouse nebulin gene sequence and the identification of cardiac nebulin. *J Mol Biol*. 328:835-46.

S8. Prado, L.G., I. Makarenko, C. Andresen, M. Kruger, C.A. Opitz, and W.A. Linke. 2005. Isoform diversity of giant proteins in relation to passive and active contractile properties of rabbit skeletal muscles. *J Gen Physiol*. 126:461-80.

SUPPLEMENTAL FIGURE LEGENDS

Supplemental Figure 1: Characterization of rabbit nebulin based on available genomic DNA sequences. A. Amino-acid sequence alignment of human (AC107052, AC009497), rabbit (Y16350, ENSOCUT00000017506), mouse (AY189120.1), and rat (XM_001056398.1) nebulin N-terminal domain (N-term) and repeat modules M1, M2, and M3. Sequences were aligned and formatted with Geneious (Company Name). Consensus sequence (top) shows residue present in the majority of the sequences. X indicates no majority present. Gaps indicated with a hyphen (-). Only residues not matching the consensus are shown for each sequence. Residues are color-coded according to charge and hydrophobicity. Similarity (bottom) between the sequences at each position; green, amber, and red indicate presence of 1, 2, or 3 different sidechains, respectively. B. Pair-wise sequence identity of N-terminal nebulin regions shown in A. The number of residues are shown in parentheses (identical/total). C) Human (blue), mouse (red), and rabbit (green) nebulin exons encoding repeat modules are highly conserved and display characteristic signature patterns along the entire sequence. X-axis: Nebulin exons encoding repeat modules. Each exon encodes one, two, or three total repeat modules and begin and end within the middle of different repeat modules. Labels indicate the repeat modules encoded by particular exons. Repeat module names were adapted from Kazmierski et al, 2003(3). Y-axis: Normalized Mass (kD) is the molecular mass per nebulin repeat module encoded by each exon. Highlighted exons: blue, human-specific; red, mouse-specific; green, incomplete rabbit sequence. Bottom scales show repeat type for each exon (simple repeats, gray; super-repeats, alternating white and black) and known regions of alternative splicing (black bars). N-terminus, N-term; C-terminus, C-term.

Supplemental Figure 2: Distributed deconvolution modeling of rabbit myofibrils stained for NebN, Tmod, and actin. (A) Thin filament models specify the distribution of fluorescence intensity (y-axis) relative to the intensity at the Z-line (Z) as a function of distance from the Z-line (x-axis). All models used are symmetric around the Z-line and are specified by three parameters (P, U, and L). P is the fluorescence intensity ratio specific to p-ends (or any localized epitope far from the Z-line) relative to the fluorescence intensity at the Z-line. U is the fluorescence intensity ratio along the thin filament relative to the Z-line. P is centered at, and U continues up to, distance ± L away from the Z-line. P-end Model: P and L respectively denote peak height and separation; U is fixed at 1 (i.e. uniform intensity along the thin filament length is equal to Z-line intensity). P-end/Z Model: Same as P-end Model except that U is not fixed which allows for reduced (or increased) uniform intensity along the thin filament relative to Z-line intensity. Uniform Model: U and L respectively determine shoulder height and width; P is fixed at 0 (i.e. no fluorescence specifically at p-ends). (B) Summary of thin filament model, their parameters, whether the parameters are optimized (Fit) or fixed (value indicated), and the set of probes for which they were used. Note: the P-end/Z Model could substitute for P-end Model for both Tmod and NebN probes; however, it was only used when background fluorescence at the Z-line was prominent which only occurred for Tmod staining (<5% of the time). (C) Myofibril intensity linescans (colored lines), modeled profiles (black lines), and residuals (points) for NebN or Tmod (red) and actin (phalloidin, green) in psoas major (PM) or diaphragm (Dia) muscle. X-axis, distance along myofibril. Y-axis, fluorescence intensity (arbitrary units). All axes are scaled identically for all four myofibrils. For clarity, only one Z-line (Z) is indicated for each myofibril linescan. Profiles, thin filament profiles (thin filament models convolved with the optimized Gaussian distribution) determined for NebN or Tmod (red) and phalloidin (green)

depict the relative fluorescence intensity for each thin filament array within the myofibril. X-axis, distance from Z-line (Z). Y-axis, fluorescence intensity (scaled individually). Based on the location of the NebN peaks, the gray region indicates the portion of the thin filament array containing nebulin. Note that Tmod fluorescence peaks extend beyond this region slightly (PM) or considerably (Dia).

Supplemental Figure 3: Correlation of nebulin isoform sizes and thin filament lengths. Graph of nebulin mol wt (kDa) versus thin filament length (nm). Solid line, ideal regression line ($y = 1.34x$) assuming each nebulin module (4.1 kDa) specifies one actin monomer (5.5 nm) starting from the center of the Z-line. Dotted line, regression line ($R^2 = 0.70$) from glycerinated rabbit myofibrils from this study (open circles). Dashed line, regression line ($y = 1.34x + 106$; $R^2 = 0.98$) for data from Kruger et al (1991) (closed circles) assuming ideal slope of 1.34 nm/kDa. Regression line of Kruger et al (1991) data without imposing the ideal slope is $y = 1.39x + 70$, ($R^2 = 0.99$).

SUPPLEMENTAL TABLES

Supplemental Table 1: Distributed Deconvolution Analysis of Rabbit Muscle Preparations

Prep.	Muscle	NebN Length ± SD	n	Tmod Length ± SD	n	ΔL Length ± SD
Cryo	PM	0.99 ± 0.04	52	1.19 ± 0.03	62	0.19 ± 0.05
	PD	1.01 ± 0.07	52	1.26 ± 0.05	52	0.25 ± 0.09
	Sol	1.00 ± 0.05	49	1.29 ± 0.09	55	0.29 ± 0.11
	Dia	1.03 ± 0.06	61	1.25 ± 0.15	37	0.22 ± 0.16
Triton	PM	0.99 ± 0.03	63	1.09 ± 0.03	70	0.10 ± 0.04
	PD	1.04 ± 0.03	46	1.18 ± 0.05	11	0.15 ± 0.06
	Sol	1.06 ± 0.03	61	1.24 ± 0.04	52	0.18 ± 0.05
	Dia	1.03 ± 0.02	57	1.21 ± 0.07	48	0.18 ± 0.07

Cryosectioned fibers (cryo); triton-extracted myofibrils (Triton); Number of linescans (n); ΔL, difference in length parameters (Tmod – NebN). All values are average ± standard deviation (SD) for one rabbit.

Supplemental Table 2: Myofibril Structural Parameters

Myofibril Structural Parameters		Value	Reference
Z-line Width	Fast-Twitch	66.6 nm	S1
	Sol	136 nm	S1
	Dia	99.4 nm	S1
Actin Subunit Repeat (Long-pitch)		5.5 nm	S2
Nebulin Module Repeat		5.5 nm	S2
Nebulin Module Size		4.1 kD	See text

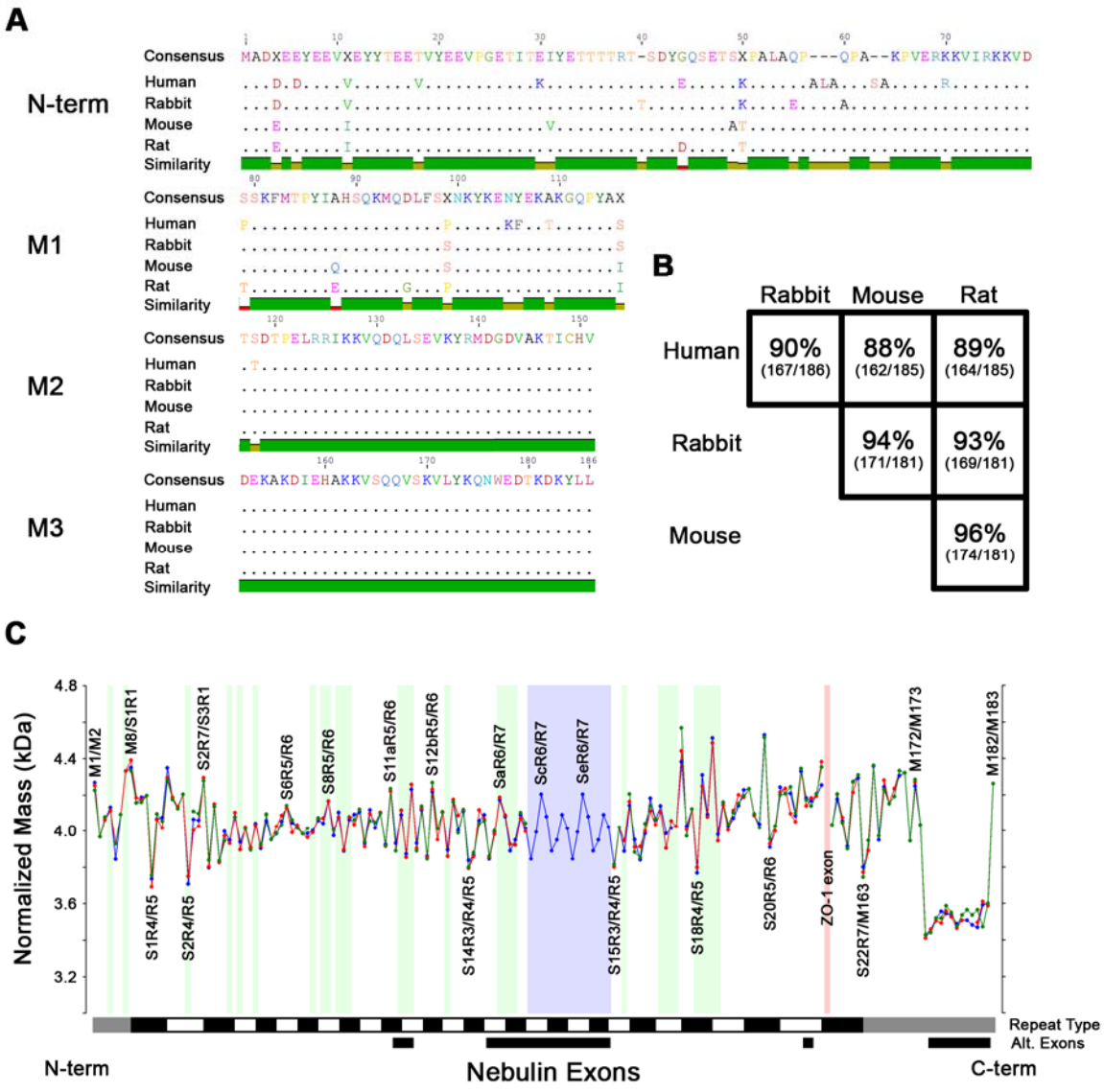

Supplemental Figure 1

Castillo et al., 2009

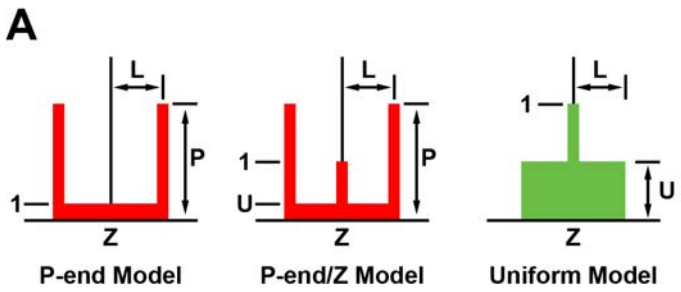

B

Model	L	U	P	Used for
P-end	Fit	1	Fit	Tmod/NebN
P-end/Z	Fit	Fit	Fit	Tmod
Uniform	Fit	Fit	0	Phalloidin

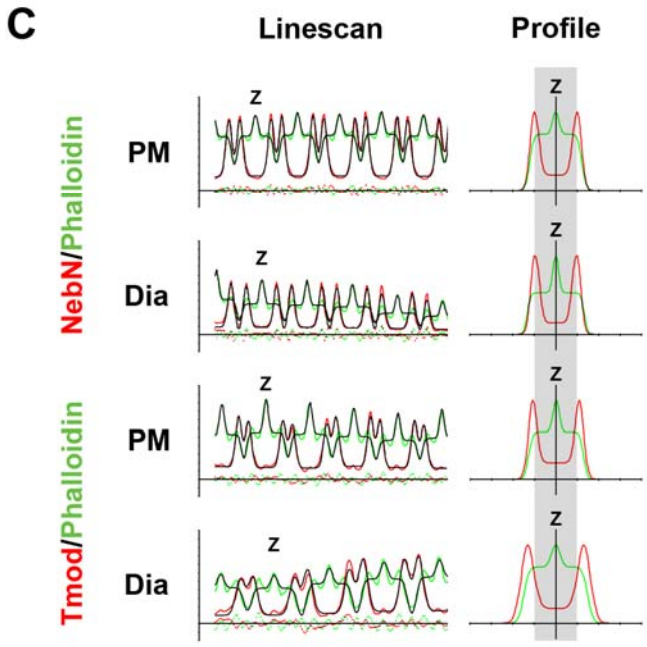

Supplemental Figure 2

Castillo et al., 2009

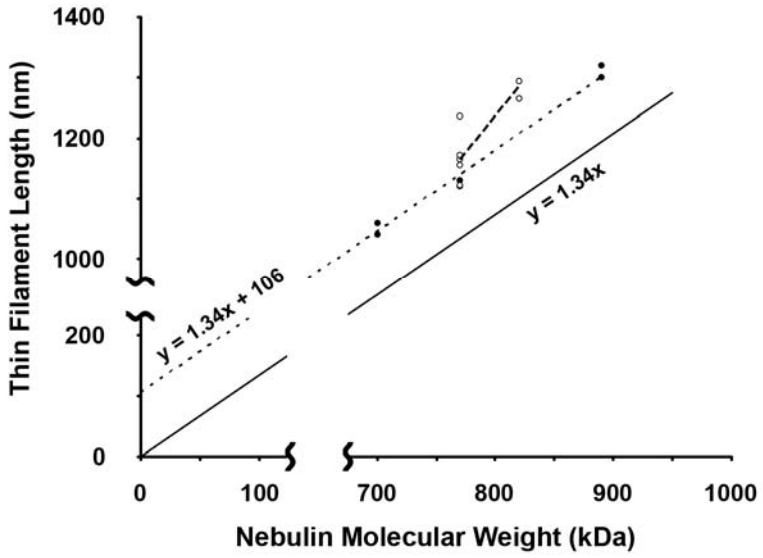

Supplemental Figure 3

Castillo et al., 2009